Propagation in Ferrite-Filled Microstrip*

MORRIS E. BRODWIN†

Summary—**The propagation constant of a ferrite-filled microstrip is measured as a function of the longitudinal static magnetic field. The results agree with the analysis by Van Trier of the infinite parallel plane waveguide filled with gyromagnetic media. The analysis is extended to anisotropies greater than 0.5. A simple relationship between propagation constant and anisotropy for the quasi-TEM mode with small spacing ($X \ll \lambda_g$) is noted. Cutoff spacings for higher modes are calculated. An apparatus for the measurement of propagation constant independently of interface reflections is described.**

Introduction

PROPAGATION of electromagnetic waves in media possessing tensor permeability has been the subject of considerable investigation. This interest has been stimulated by the development of low-loss ferromagnetic materials called ferrites which easily exhibit electron spin resonance. Van Trier[1] has solved the case of a circular waveguide filled with ferrite and biased in the direction of propagation. He also analyzed in some detail the ferrite-filled parallel plane waveguide with a longitudinal magnetizing field. The case of circular waveguide filled with ferrite material and magnetized in the direction of propagation has also been treated by Kales.[2] Lax[3] has investigated the rectangular waveguide partially filled with ferrite and transversely magnetized.

The principal experimental work with ferrites has been largely restricted to the circular and rectangular waveguide structures. The only reported work in stripline waveguide is that of Fix[4] and Arditi.[5] Fix[4] placed the ferrite material between two coupled strip-lines. When the stripline fields are in phase quadrature, a circularly polarized wave is produced in the fringing region. With a longitudinal static magnetic field, the structure exhibited nonreciprocal effects. Arditi[5] symmetrically located the ferrite slab in a microstrip structure and took measurements of relative attenuation and phase shift. No attempt was made to explain quantitatively the experimental results.

The problem treated in this paper is the determination of the applicability of the parallel plane waveguide analysis to the wide strip ferrite-filled microstrip. More specifically, we attempt to determine how closely the variation in propagation constant with longitudinal magnetic field for microstrip follows the variation predicted by a parallel plane analysis of the quasi-TEM mode. The analysis of Van Trier is extended to include high values of anisotropy.

A simple relationship between anisotropy and propagation constant is derived for the quasi-TEM mode. Experiments are described for determining the propagation constant independent of the ferrite interface reflections.

Analysis

We consider the medium to be a lossless dielectric with a tensor permeability

$$(\mu) = \begin{bmatrix} \mu_1 & -i\mu_2 & 0 \\ i\mu_2 & \mu_1 & 0 \\ 0 & 0 & \mu_3 \end{bmatrix}. \tag{1}$$

If the ferrite is demagnetized $\mu_3 = \mu_1$ and $\mu_2 = 0$; at saturation $\mu_3 = \mu_0$.

We commence with a cartesian coordinate system with the biasing magnetic field in the z direction. The fields are assumed to be of the form $u(x, y)e^{i\omega t - \Gamma z}$. Following Van Trier, the substitution of the tensor permeability into Maxwell's equations yields the coupled wave equations

$$\nabla_t^2 H_z + aH_z + bE_z = 0 \tag{2a}$$

and

$$\nabla_t^2 E_z + cE_z + dH_z = 0 \tag{2b}$$

where

$$a = \Gamma^2 + \omega^2 \epsilon \mu_1$$

$$b = -\omega\epsilon \frac{\mu_2}{\mu_1} \Gamma$$

$$c = \Gamma^2 + \omega^2 \epsilon \mu_1 \left[1 - \left(\frac{\mu_2}{\mu_1} \right)^2 \right]$$

$$d = \omega \mu_2 \Gamma.$$

By means of a change in variable

$$E_z = \alpha_1 + \alpha_2 \tag{3a}$$

$$H_z = K_1 \alpha_1 + K_2 \alpha_2 \tag{3b}$$

where K_1 and K_2 are chosen to uncouple the equations in α_1 and α_2.

* Manuscript received by the PGMTT, June 3, 1957; revised manuscript received, October 10, 1957. This research was supported by the USAF through the Office of Scientific Research of ARDC.

† Radiation Lab., The Johns Hopkins University, Baltimore, Md.

[1] A. A. Van Trier, "Guided electromagnetic waves in antisotropic media," *Appl. Sci. Res.*, Vol. B-3, pp. 305–371; December, 1953.

[2] M. L. Kales, "Modes in waveguide containing ferrites," *J. Appl. Phys.*, vol. 24, pp. 604–608; May, 1953.

[3] B. Lax, K. J. Button, and L. M. Roth, "Ferrite Phase Shifters in Rectangular Waveguide," M.I.T., Cambridge, Mass., Tech. Memo. No. 49; November, 1953.

[4] O. W. Fix, "A balanced-stripline isolator," 1956 IRE Convention Record, pt. 5, pp. 99–105.

[5] M. Arditi, "Experimental determination of the properties of microstrip components," 1953 IRE Convention Record, pt. 10, pp. 27–37.

Eqs. (2a) and (2b) can be written as

$$\nabla_t^2\alpha_i + \sigma_i^2\alpha_i = 0 \qquad i = 1, 2 \tag{4}$$

where

$$\sigma_{1,2r}^2 = \frac{\sigma_{1,2}^2}{\omega^2\epsilon\mu_1} = \Gamma_r^2 + 1 - \frac{1}{2}\left(\frac{\mu_2}{\mu_1}\right)^2 \pm \left\{\left(\frac{\mu_2}{\mu_1}\right)\left[\left(\frac{\mu_2}{2\mu_1}\right)^2 - \Gamma_r^2\right]^{1/2}\right\}. \tag{5}$$

Application of the boundary condition, $E_{\tan} = 0$ yields

$$\alpha_1 + \alpha_2 = 0 \tag{6a}$$

and

$$\delta_2\left[\frac{\partial}{\partial\tau}(\sigma_2^2\alpha_1 + \sigma_1^2\alpha_2)\right] - \delta_1\left[\frac{\partial}{\partial\eta}(\sigma_2^2\alpha_1 + \sigma_1^2\alpha_2)\right] + [\delta_1 a + \delta_3 d]\left[\frac{\partial}{\partial\eta}(\alpha_1 + \alpha_2)\right] = 0 \tag{6b}$$

where

$$\delta_1 = i\omega[\omega^2\epsilon(\mu_2^2 - \mu_1^2) - \mu_1\Gamma^2]/\delta$$
$$\delta_2 = \omega\mu_2\Gamma^2/\delta$$
$$\delta_3 = -i\omega^2\epsilon\mu_2\Gamma/\delta$$
$$\delta = \{\Gamma^2 + \omega^2\epsilon(\mu_1 + \mu_2)\}\{\Gamma^2 + \omega^2\epsilon(\mu_1 - \mu_2)\}.$$

$\partial/\partial\tau$, $\partial/\partial\eta$ are the tangential and normal derivatives. The symmetrical and antisymmetrical solutions of (4) are substituted into the boundary conditions, (6a) and (6b), and the resulting expressions evaluated on the boundary of Fig. 1. This process leads to two equations which are implicit relations involving the propagation constant and the anisotropy, μ_2/μ_1.

Restricting the discussion to the antisymmetric solutions leads to the following relation involving Γ_r.

$$O_1P_2 - O_2P_1 = O \tag{7}$$

where

$$O_{1,2} = \omega^2\mu_1\sqrt{\epsilon\mu_1}\sigma_{2,1r}[1 - U\sigma_{1,2r}^2]$$

$$U = \frac{1 + \Gamma_r^2 - \left(\frac{\mu_2}{\mu_1}\right)^2}{(\Gamma_r^2 + 1)^2 - \left(\frac{\mu_2}{\mu_1}\right)^2}$$

$$P_{1,2} = [e^{i\sigma_{1,2r}X_{or}} + e^{-i\sigma_{1,2r}X_{or}}][e^{i\sigma_{2,1r}X_{or}} - e^{-i\sigma_{2,1r}X_{or}}]$$

where

$$X_{or} = X_o\omega\sqrt{\epsilon\mu_1}.$$

Values of the propagation constant Γ_r are determined by choosing a suitable spacing and anisotropy and varying the propagation constant until the left-hand side of (7) is zero. Eq. (7) applies to the odd quasi-TE modes, and even quasi-TM modes as well as the quasi-TEM mode. The ambiguity between a correct value of propagation constant and the mode with which it is related is resolved by starting the calculations with small anisotropy. The assumed values of propagation constant are chosen in the immediate region of the corresponding isotropic mode.

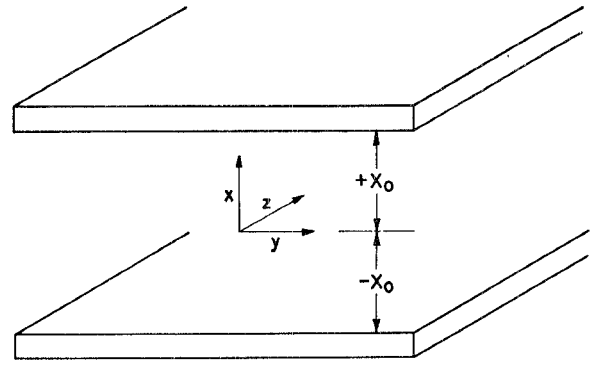

Fig. 1—Coordinates for parallel plane waveguide.

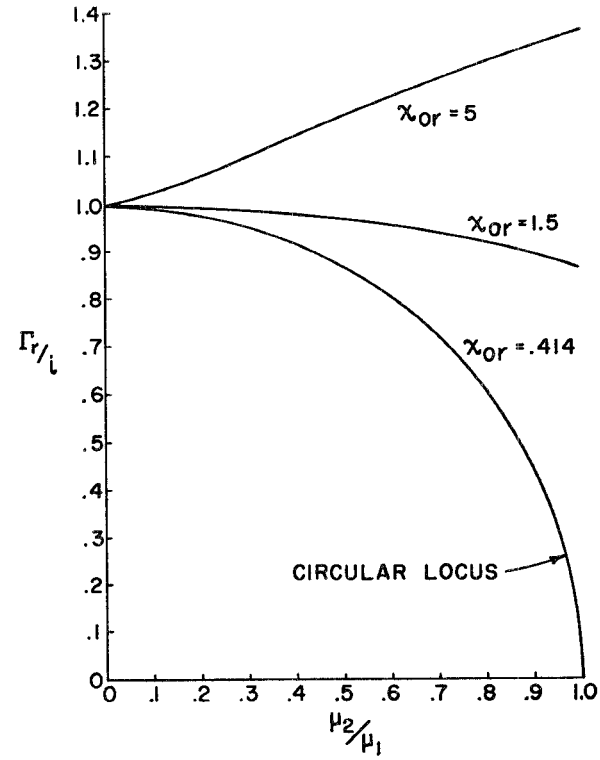

Fig. 2—Propagation constant vs anisotropy—quasi-TEM.

The propagation constant, Γ_r, for the quasi-TEM mode has been calculated for a range of X_{or} and μ_2/μ_1, Fig. 2. The curve $X_{or} = 1.5$ corresponds to the behavior of the waveguide with approximately $\lambda/2$ spacing between the parallel planes. The wavelength, λ, is the intrinsic wavelength associated with the material. For spacings less than $\lambda/2$, the dependence of Γ_r on μ_2/μ_1 approaches a circular locus. Additional curves ($X_{or} = 0.1$, 0.2, 0.3) were calculated but are not displayed since they overlap the $X_{or} = 0.414$ curve. This result is useful for design purposes since it relates the propagation constant and anisotropy in a simple fashion.

For small spacing ($X_{or} \leq 0.414$)

$$\left(\frac{\mu_2}{\mu_1}\right)^2 + \left(\frac{\Gamma_r}{i}\right)^2 = 1. \tag{8}$$

The error between points calculated with (8) and points laboriously calculated with (7) is less than 0.9 per cent for small spacing.

For large spacing ($X_{or}=5$), the trend is reversed. The propagation constant increases with anisotropy instead of decreasing. This peculiar behavior implies that the waveguide acts as a slow wave structure for large spacing and a fast wave structure for small spacing.

When the anisotropy is unity, the corresponding value of the propagation constant is undetermined. This result arises from the behavior of U as $\mu_2/\mu_1 \rightarrow 1$ and $\Gamma_r \rightarrow 0$. U can have any value depending upon the manner in which the variables approach the limit. The trend of the values for anisotropy less than unity and small spacing indicates that the propagation constant tends toward zero as the anisotropy tends toward unity. This result has been verified experimentally. For an anisotropy greater than unity, values of the propagation constant cannot be determined from (7) or its symmetric counterpart. For example, Fig. 3 is a plot of $O_1P_2 - O_2P_1$ vs Γ_r/i with $\mu_2/\mu_1 = 2$, $X_{or}=0.414$. At low values of Γ_r/i, the function is imaginary and negative. As Γ_r/i increases, the functions tend toward infinity. At a larger value of Γ_r/i, the function starts again with negative real values. Since the function does not pass through zero, the waveguide is beyond cutoff for anisotropies greater than unity.

The critical spacings for the higher modes is determined by setting Γ_r equal to zero in (7) and solving for X_{or}'.

$$X_{or}' = \frac{n\pi}{2\left[1 - \left(\frac{\mu_2}{\mu_1}\right)^2\right]^{1/2}} \quad \text{even } n. \tag{9}$$

When the process is repeated for the symmetric solutions, the same result is obtained, but with odd n. The mode titles are assigned by comparing the result with the solutions for the isotropic case.

The critical spacing for the quasi-TM_n modes are shown in Fig. 4. The critical spacings for the quasi-TE modes are the same as the critical spacings for the quasi-TM modes. This degeneracy in the isotropic case is preserved in the anisotropic case. If we choose a spacing much smaller than $\lambda/2$ to insure that the quasi-TEM mode is the only propagating mode, then an increase in anisotropy does not permit the propagation of higher modes. This result follows from the increase in critical spacing with increasing anisotropy.

Experimental Procedure

The experimental problem is to determine how closely the ferrite-filled microstrip approximates the theoretical predictions of the parallel plane waveguide. The technique consists of placing a ferrite-filled microstrip in a longitudinal magnetic field and determining the relationship between the propagation constant and the magnetic field. In order to approach as closely as possible the parallel plane case, the upper strip width is approximately $\lambda/2$. The microstrip geometry is shown in Fig. 5.

The principal experimental difficulties are caused by the necessity for placing the microstrip within a solenoid. The space limitations prohibit the use of direct field sampling techniques. If measurements are taken external to the ferrite section, the usual phase sensitive bridges are subject to errors caused by variable dielectric-ferrite interface reflections. To avoid these difficulties, a perturbation technique was employed. This apparatus consists of a movable small reflector mounted

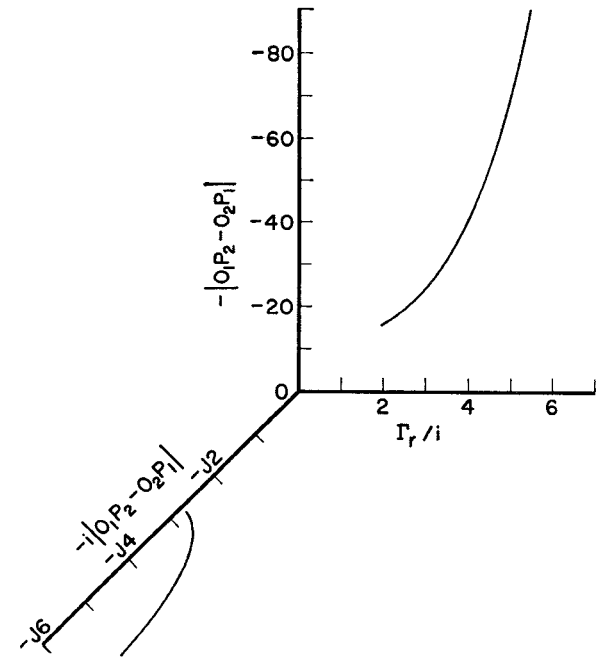

Fig. 3—Behavior for $(\mu_2/\mu_1) > 1$.

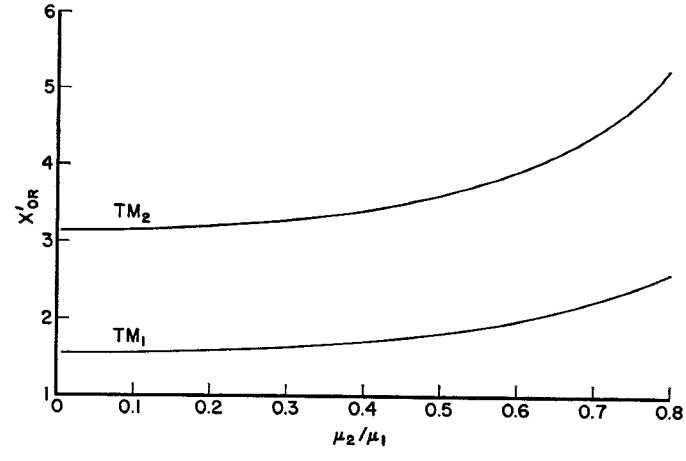

Fig. 4—Critical spacings for the higher modes.

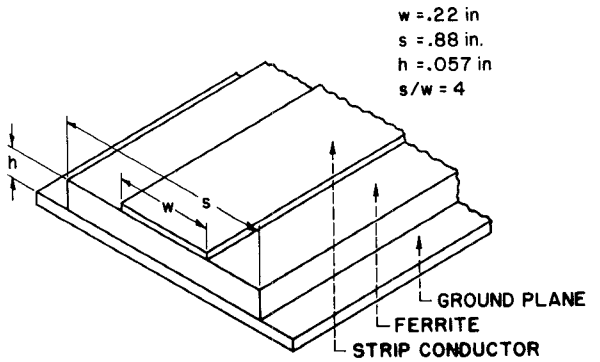

Fig. 5—Microstrip geometry.

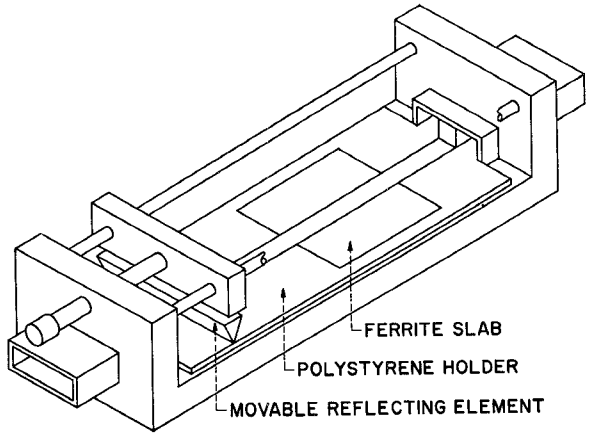

Fig. 6—Apparatus for perturbation technique.

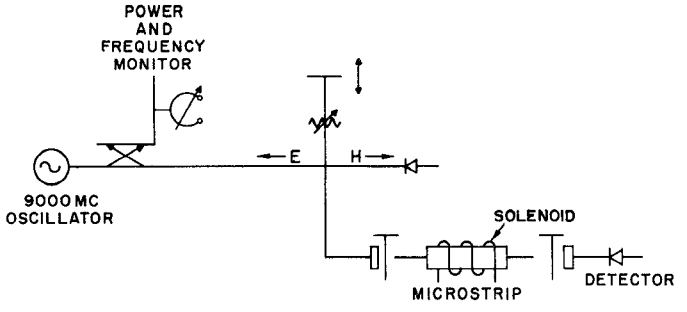

Fig. 7—Phase sensitive bridge.

close to the upper plane of the stripline, Fig. 6. The metal wedge reflects part of the fringing field, and the resultant reflections are determined by a microwave bridge, Fig. 7. The position of the reflecting element is controlled by means of a lead screw. When the reflecting element is displaced by $\lambda_g/2$, the total reflection from the sample is unchanged. In this manner, the interface reflections as well as any reflections from the transitions do not affect the measurement.

The samples were prepared in the following manner. To insure that higher modes would not propagate, the spacing between upper and lower planes of the stripline was chosen as 0.057 inch for a dielectric constant of 7.3. Rectangular samples, $\frac{7}{8}\times 1\frac{1}{2}\times 0.057$ inch, were prepared and fitted into a polystyrene slab. The dielectric sample holder was cut with linear tapers at each end to reduce reflections from the transitions. The upper and lower conducting planes were prepared by spraying silver paint on the masked sample holder and electroplating a 50-micron copper film. The ferrite employed in these experiments was "R-1," manufactured by General Ceramic and Steatite. The dielectric constant of the ferrite, $\epsilon = 7.3$, was measured by a standard waveguide technique and by the microstrip method previously described. This value is considerably different from the nominal value of 13. The discrepancy is possibly due to the large batch to batch variation of early ferrite materials.

Experimental Results

The phase constant was measured for magnetic fields between 0 and 1700 oersteds. The results of these measurements are shown in Fig. 8. To determine the relative transmission loss, a matched detector was placed at the output transition and the detected energy was noted for different values of applied field. These results are shown in Fig. 9. No significant difference in phase constant or insertion loss was noted when the experiments were repeated with a reversed magnetic field.

Discussion

The variation of phase constant with applied magnetic field agrees, qualitatively, with the predicted behavior of the ferrite-filled parallel plane waveguide. Starting with zero applied field, the phase constant should decrease as the anisotropy is increased, Fig. 2, $X_{or} = 0.414$. At the magnetic field at which the anisotropy is unity, the propagation constant is zero. Above this point, the ferrite section is beyond cutoff. The experimental data shows that the phase constant decreased until a field of 1025 oersteds was reached. The transmission data indicates that the stripline was cut off at 1025 oersteds. The maximum field was 1700 oersteds. The theory, as previously developed, cannot predict losses since it was assumed that μ_1 and μ_2 are real quantities. Consequently, the propagation constant is a pure imaginary and attenuation is not expected. The general trend of the relative transmission, Fig. 9 shows an increase in loss with an increase in magnetic field. From 1025 to 1700 oersteds, the readings remained constant. This small residual transmission is attributed to leakage between the microstrip-waveguide transitions. The fine variation in transmission is produced by the changing wavelength in conjunction with the interface reflections. This is the typical interference phenomenon observed with any resonant structure with varying phase shift.

It is possible to obtain a theoretical expression for the variation of phase constant as a function of the applied magnetic field subject to the following simplifying assumptions:

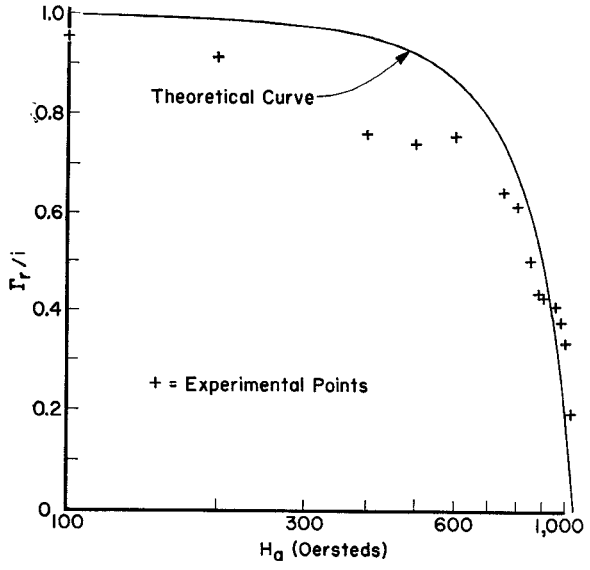

Fig. 8—Phase constant vs applied field.

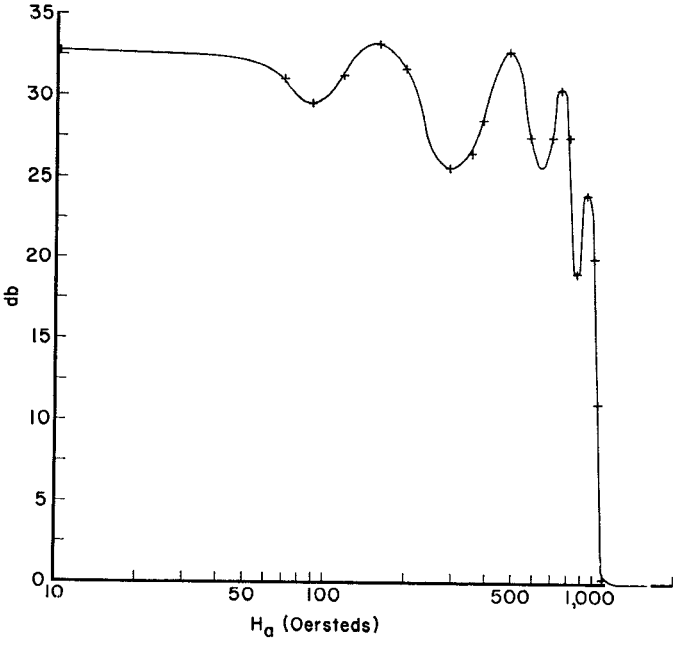

Fig. 9—Relative transmission vs applied field.

1) The static field inside the sample is assumed to be homogeneous. The effects of demagnetization can be expressed by a demagnetizing factor. Since the sample is a rectangular parallelepiped, the internal field is actually inhomogeneous, but this effect is neglected.

2) The magnetic behavior can be expressed by a constant magnetic susceptibility. This assumption is approximately correct only in the region of saturation.

With these assumptions, a relationship between μ_2/μ_1 and the applied field, H_a, can be determined.

The anisotropy is related to the applied field by (see Appendix)

$$\frac{\mu_2}{\mu_1} = \frac{\omega\gamma K(1 + NK)H_a}{\gamma^2 H_a^2(1 + K) - \omega^2(1 + NK)^2} \tag{10}$$

where

ω = angular frequency
γ = gyromagnetic ratio
K = magnetic susceptibility
N = demagnetization factor
H_a = applied static magnetic field.

If the ferrite slab can be represented by an equivalent ellipsoid of revolution, the demagnetization factor can be calculated. With the dimensions of the slab used in the experiments, $N = 3 \times 10^{-3}$. In the region of saturation, K is on the order of unity and $NK \ll 1$. The demagnetization effects, therefore, are neglected. The relationship between anisotropy and H_a is then given by

$$\frac{\mu_2}{\mu_1} = \frac{\omega\gamma K H_a}{\gamma^2 H_a^2(1 + K) - \omega^2}. \tag{11}$$

The susceptibility is determined by assuming that cutoff occurs when the anisotropy is unity and solving (11) for K_c for cutoff at 1025 oersteds. The calculated value for K_c is 2.45. When this value of K is substituted into (11), the resultant relationship between μ_2/μ_1 and H_a represents the theoretical behavior of the anisotropy with the applied field. To determine Γ_r/i as a function of H_a, (11) is substituted into (8).

$$\left(\frac{\Gamma_r}{i}\right)^2 = 1 - \left[\frac{\omega\gamma K_c H_a}{\gamma^2 H_a^2(1 + K_c) - \omega^2}\right]. \tag{12}$$

This equation was employed for drawing the theoretical curve of Fig. 8.

In general, the theoretical curve follows the trend of the data. The principal discrepancy is in the region between 100 and 600 oersteds, where the experimental points are lower than the predicted value. This discrepancy may be a result of the assumption that K remained constant. In the low-field region, where the material is not saturated, K is larger than the chosen value. Increasing K decreases the right-hand side of (12) and would yield a smaller value for Γ_r/i.

A question arises as to how much of the insertion loss is due to a cutoff effect and how much is due to radiation from the microstrip. With this experimental technique, it is not possible to distinguish between the two effects. However, the fact that the experimental points agree very closely with the theoretical values in the region of large insertion loss might indicate that the cutoff effect predominates.

Appendix

The relationship between the applied magnetic field and anisotropy is derived from Polder's equations[6] for μ_1 and μ_2:

[6] D. Polder, "On the theory of ferromagnetic resonance," *Phil. Mag.*, vol. 40, pp. 99–115; January, 1949.

$$\mu_1 = \mu_0\left[1 - \frac{\gamma M\omega_0}{\omega_0^2 - \omega^2}\right] \quad (1)$$

$$\mu_2 = \frac{\mu_0\gamma M\omega}{\omega_0^2 - \omega^2} \quad (2)$$

where

$\omega_0 = \gamma H_1$
H_1 = internal static magnetic field
μ_0 = permeability of free space
γ = gyromagnetic ratio
M = magnetic polarization density
ω = angular frequency.

The anisotropy, μ_2/μ_1, is related to the internal field by

$$\frac{\mu_2}{\mu_1} = \frac{\gamma M\omega}{\omega_0^2 - \gamma M\omega_0 - \omega^2}. \quad (3)$$

Assuming a demagnetization factor N, the internal field is related to the external field. Expressing the magnetic polarization density in terms of a magnetic susceptibility K, and the internal field, the final equation is

$$\frac{\mu_2}{\mu_1} = \frac{\omega\gamma K(1 + NK)H_a}{\gamma^2 H_a^2(1 + K) - \omega^2(1 + NK)^2}. \quad (4)$$

ACKNOWLEDGMENT

The author is indebted to Dr. D. D. King, Dr. M. I. Aissen, and other colleagues for their stimulating discussions and helpful criticism.

An Improved Method for the Determination of Q of Cavity Resonators*

AMARJIT SINGH†

Summary—The various Q factors and circuit efficiency of a cavity resonator can be evaluated from standing-wave measurements on a transmission line or waveguide coupled to the resonator. In the usual method, measurement errors near the half-power points have an unduly large influence on the result. This paper describes a method in which this type of error is avoided.

In the new method, vswr and position of minimum at various frequencies are plotted on a Smith chart and a circle is drawn through the points. This circle is suitably rotated around the center of the chart and a value of equivalent susceptance is read off for each frequency. The graph of susceptance vs frequency is a straight line, from whose slope the Q factors are evaluated.

The underlying theory of the above method is discussed and typical experimental results are presented. Charts of parameters required in the calculations are given.

INTRODUCTION

THE measurement of the Q of cavity resonators finds many applications in the field of microwave electronics, as well as in physical research. Several methods of determination of Q have been developed.[1–3] Among these is the method involving measurements on standing waves in a transmission line or waveguide coupled to the resonator. The method is not a quick one; however, it has the advantage of supplying the most complete information about the resonator and the coupling system. The losses inside the cavity, the losses in the coupling system, and the power coupled into the transmission line, can all be separated out.[4] This information is indispensable in such applications as design of microwave tubes, where the circuit efficiency is an important parameter.

After data have been obtained on the variation of vswr and the position of voltage minimum in the line as functions of frequency, it is possible to determine the frequencies which correspond to the half-power points. The Q factors can then be evaluated. The previously developed methods of obtaining the half-power frequencies employ a curve showing vswr vs frequency or one showing the position of the minimum vs frequency. On these curves, one reads off the frequencies which correspond to certain values of vswr or of shift in the position of the minimum. It is to be noted that these curves are not geometrically simple ones, and that any errors in the observations near the half-power points have a large influence on the result. In fact, a discrepancy may be observed between the results obtained

* Manuscript received by the PGMTT, June 19, 1957; revised manuscript received, August 6, 1957.
† Central Electronics Engineering Res. Inst., Pilani, India. Formerly with the Natl. Physical Lab. of India, New Delhi, India.
[1] C. G. Montgomery, "Technique of Microwave Measurements," McGraw-Hill Book Co., Inc., New York, N. Y.; 1947.
[2] H. M. Barlow and A. L. Cullen, "Microwave Measurements," Constable and Co., London, Eng.; 1950.
[3] M. Wind and H. Rapaport, "Handbook of Microwave Measurements," Polytechnic Institute of Brooklyn, Brooklyn, N. Y., vols. I and II; 1955.
[4] L. Malter and G. R. Brewer, "Microwave Q measurements in the presence of series losses," *J. Appl. Phys.*, vol. 20, pp. 918–925; October, 1949.